Applied Mathematics & Information Sciences **3**(1) (2009), 25–44
– An International Journal

Axi-Symmetric Vibrations in a Microstretch Viscoelastic Plate

Rajneesh Kumar[1] and Geeta Partap[2]

[1]Department of Mathematics, Kurukshetra University, Kurukshetra, Haryana, India -136119

Email Address: rajneesh_kuk@rediffmail.com

[2]Department of Mathematics, Dr. B. R. Ambedkar National Institute of Technology

Jalandhar, Punjab, India - 144011

Email Address: gp.recjal@gmail.com

Received January 8, 2008; Revised May 13, 2008

The propagation of axi-symmetric vibrations in a homogeneous isotropic microstretch viscoelastic plate subjected to stress free conditions is investigated. The secular equations for homogeneous isotropic microstretch viscoelastic plate for symmetric and skew symmetric wave modes propagation are derived. The special cases such as short wavelength and regions of secular equations are deduced and discussed. The dispersion curves, amplitudes of displacement components, microrotation and microstretch for symmetric and skew symmetric modes are computed numerically and presented graphically.

Keywords: Microstretch viscoelastic plate, secular equations, phase velocity, attenuation coefficients.

1 Introduction

A micropolar continuum is a collection of interconnected particles in the form of small rigid bodies undergoing both translational and rotational motions. Typical examples of such materials are granular media and multi-molecular bodies whose microstructures act as an evident part in their macroscopic responses. Rigid chopped fibres, elastic solids with rigid granular inclusions and other industrial materials such as liquid crystals are examples of such materials.

Eringen [6] extended his work to include the effect of axial stretch during the rotation of molecules and developed the theory of micropolar elastic solid with stretch. The material points in this continuum possess not only classical translational degree of freedom represented by the deformation vector field but also intrinsic rotations and an intrinsic axial stretch. The difference between these solids and micropolar elastic solids stems from the

presence of scalar microstretch and a vector first moment. Microstretch continuum is a model for Bravais lattice with basis on the atomic level and two phase dipolar solids with a core on the macroscopic level. Composite materials reinforced with chopped elastic fibres, porous media whose pores are filled with gas or inviscid liquid, asphalt or other elastic inclusions and solid-liquid crystals etc. are examples of microstretch solids.

Liu and Hu [19] investigated the inclusion problem of microstretch. Svanadze [21] constructed fundamental solution of the system of equations of steady oscillations in the theory of microstretch elastic solids. De Cicco [2] investigated the stress concentration effects in microstretch elastic bodies. Kumar *et al.* [16] discussed the axisymmetric problem in microstretch. Kumar *et al.* [17] investigated plane strain problem in microstretch elastic solid. Kumar and Partap [12] investigated reflection of plane waves in a heat flux dependent microstretch thermoelastic solid half spaces.

Eringen [5] extended the theory of micropolar elasticity to obtain linear constitutive theory for micropolar material possessing internal friction. A problem on micropolar viscoelastic waves has been discussed by McCarthy and Eringen [20]. Biswas *et al.* [1] studied the axisymmetric problems of wave propagation under the influence of gravity in a micropolar viscoelastic semi-infinite medium when a time varying axisymmetric loading has been applied on the surface of the medium. De Cicco and Nappa [3] discussed the problem of Saint Venant's principle for micropolar viscoelastic bodies. Kumar and Singh [14] studied reflection of plane waves at a planar viscoelastic micropolar interface.

Recently EI-Karamany [4] studied uniqueness and reciprocity theorems in a generalized linear micropolar thermoviscoelasticity. Kumar *et al.* [11] studied Lamb's plane problem in a micropolar viscoelastic half space with stretch. Kumar [10] discussed wave propagation in micropolar viscoelastic generalized thermoelastic solid. Kumar and Singh [15] studied elastodynamics of an axisymmetric problem in microstretch viscoelastic solid.
The present investigation is aimed to study the propagation of axi-symmetric vibrations in an infinite homogeneous, isotropic microstretch viscoelastic plate of thickness 2d.

2 Basic Equations

The equations of motion and the constitutive relations in a microstretch elastic solid without body forces, body couples and stretch force given by Eringen [7] are

$$(\lambda + 2\mu + K)\nabla(\nabla \cdot \vec{u}) - (\mu + K)\nabla \times \nabla \times \vec{u} + K\nabla \times \vec{\phi} + \lambda_0 \nabla \phi^* = \rho \frac{\partial^2 \vec{u}}{\partial t^2}, \quad (2.1)$$

$$(\alpha + \beta + \gamma)\nabla(\nabla \cdot \vec{\phi}) - \gamma\nabla \times (\nabla \times \vec{\phi}) + K\nabla \times \vec{u} - 2K\vec{\phi} = \rho j \frac{\partial^2 \vec{\phi}}{\partial t^2}, \quad (2.2)$$

$$\alpha_0 \nabla^2 \phi^* - \lambda_1 \phi^* - \lambda_0 \nabla \cdot \vec{u} = \frac{1}{2}\rho j_0 \frac{\partial^2 \phi^*}{\partial t^2}, \quad (2.3)$$

$$t_{ij} = (\lambda_0\phi^* + \lambda u_{r,r})\delta_{ij} + \mu(u_{i,j} + u_{j,i}) + K(u_{j,i} - \epsilon_{ijr}\phi_r), \tag{2.4}$$

$$m_{ij} = \alpha\phi_{r,r}\delta_{ij} + \beta\phi_{i,j} + \gamma\phi_{j,i} + b_0\epsilon_{mji}\phi^*_{,m}, \tag{2.5}$$

$$\lambda^*_i = \alpha_0\phi^*_{,i} + b_0\epsilon_{ijm}\phi_{j,m} \tag{2.6}$$

where $\lambda, \mu, \alpha, \beta, \gamma, K, \alpha_0, \lambda_0, \lambda_1, b_0$ are material constants, ρ is the density, j is the microinertia, j_0 is the microinertia of microelement, t_{ij} components of force stress tensor, m_{ij} components of couple stress tensor, $\vec{u} = (u_r, u_\theta, u_z)$ is the displacement vector, $\vec{\phi} = (\phi_r, \phi_\theta, \phi_z)$ is the microrotation vector, λ^*_i is the microstress tensor, ϕ^* is the scalar point microstretch function,δ_{ij} is Kronecker delta. The comma notation denotes spatial derivatives.

Assuming that the viscoelastic nature of the material is described by Kumar and Singh [15] model of linear viscoelasticity, we replace the microstretch elastic constants $\lambda, \mu, K, \alpha, \beta, \gamma, \alpha_0, \lambda_0, b_0$, and λ_1 by $\lambda_I, \mu_I, K_I, \alpha_I, \beta_I, \gamma_I, \alpha_{0I}, \lambda_{0I}, b_{0I}$, and λ_{1I}, where

$$\lambda_I = \lambda + \lambda_v\frac{\partial}{\partial t},\ \mu_I = \mu + \mu_v\frac{\partial}{\partial t},\ K_I = K + K_v\frac{\partial}{\partial t},\ \alpha_I = \alpha + \alpha_v\frac{\partial}{\partial t},\ \beta_I = \beta + \beta_v\frac{\partial}{\partial t},$$

$$\gamma_I = \gamma + \gamma_v\frac{\partial}{\partial t},\ \alpha_{0I} = \alpha_0 + \alpha_{0v}\frac{\partial}{\partial t},\ \lambda_{0I} = \lambda_0 + \lambda_{0v}\frac{\partial}{\partial t},\ \lambda_{1I} = \lambda_1 + \lambda_{1v}\frac{\partial}{\partial t},\ b_{0I} = b_0 + b_{0v}\frac{\partial}{\partial t}.$$

Here $\lambda_v, \mu_v, K_v, \alpha_v, \beta_v, \gamma_v, \alpha_{0v}, \lambda_{0v}, \lambda_{1v}, b_{0v}$ are viscosity constants in Eqs. (2.1)–(2.6). We obtain

$$(\lambda_I + 2\mu_I + K_I)\nabla(\nabla\cdot\vec{u}) - (\mu_I + K_I)\nabla\times\nabla\times\vec{u} + K_I\nabla\times\vec{\phi} + \lambda_{0I}\nabla\phi^* = \rho\frac{\partial^2\vec{u}}{\partial t^2}, \tag{2.7}$$

$$(\alpha_I + \beta_I + \gamma_I)\nabla(\nabla\cdot\vec{\phi}) - \gamma_I\nabla\times(\nabla\times\vec{\phi}) + K_I\nabla\times\vec{u} - 2K_I\vec{\phi} = \rho j\frac{\partial^2\vec{\phi}}{\partial t^2}, \tag{2.8}$$

$$\alpha_{0I}\nabla^2\phi^* - \lambda_{1I}\phi^* - \lambda_{0I}\nabla\cdot\vec{u} = \frac{1}{2}\rho j_0\frac{\partial^2\phi^*}{\partial t^2}, \tag{2.9}$$

$$t_{ij} = (\lambda_{0I}\phi^* + \lambda_I u_{r,r})\delta_{ij} + \mu_I(u_{i,j} + u_{j,i}) + K_I(u_{j,i} - \epsilon_{ijr}\phi_r), \tag{2.10}$$

$$m_{ij} = \alpha_I\phi_{r,r}\delta_{ij} + \beta_I\phi_{i,j} + \gamma_I\phi_{j,i} + b_{0I}\epsilon_{mji}\phi^*_{,m}, \tag{2.11}$$

$$\lambda^*_i = \alpha_{0I}\phi^*_{,i} + b_{0I}\epsilon_{ijm}\phi_{j,m}. \tag{2.12}$$

3 Formulation of the Problem

We consider a homogeneous isotropic microstretch viscoelastic plate of thickness $2d$. The plate is axi-symmetric with respect to z-axis as the axis of symmetry. The origin of the co-ordinate system (r, θ, z) is taken at any point in the middle surface of the plate and z-axis normal to it along the thickness. We take r–z plane as the plane of incidence.

For two dimensional problem, we take

$$\vec{u} = (u_r, 0, u_z) \quad \text{and} \quad \vec{\phi} = (0, \phi_\theta, 0).$$

We define the non-dimensional quantities

$$r' = \frac{\omega^* r}{c_1}, z' = \frac{\omega^* z}{c_1}, u'_r = \frac{\omega^*}{c_1} u_r, u'_z = \frac{\omega^*}{c_1} u_z, t' = \omega^* t, \phi'_\theta = \frac{{\omega^*}^2 j}{c_1^2}\phi_\theta, \phi^{*'} = \frac{{\omega^*}^2 j}{c_1^2}\phi^*,$$

$${\omega^*}^2 = \frac{K_I}{\rho j},\ \omega'^2 = \frac{\omega^2}{{\omega^*}^2},\ t'_{ij} = \frac{1}{\lambda_I} t_{ij},\ m'_{ij} = \frac{\omega^* m_{ij}}{\lambda_I c_1},\ \lambda_i^{*'} = \frac{\omega^* \lambda_i^*}{c_1 \lambda_I},\ p = \frac{K_I}{\rho c_1^2},\ \delta^2 = \frac{c_2^2}{c_1^2},$$

$$\delta_2^2 = \frac{c_1^2}{c_4^2},\ \delta_3^2 = \frac{\lambda_{0I}}{K_I},\ {\delta^*}^2 = \frac{K_I}{\rho c_4^2},\ \delta_4^2 = \frac{\lambda_{1I} c_1^2}{\alpha_{0I} {\omega^*}^2},\ \delta_5^2 = \frac{\lambda_{0I} j}{\alpha_{0I}},\ \delta_6^2 = \frac{\rho c_1^2 j_0}{2\alpha_{0I}}. \tag{3.1}$$

where

$$c_1^2 = \frac{\lambda_I + 2\mu_I + K_I}{\rho},\ c_2^2 = \frac{\mu_I + K_I}{\rho},\ c_4^2 = \frac{\gamma_I}{\rho j},$$

ω^* is the characteristic frequency of the medium, c_1 and c_2 are respectively the longitudinal and shear wave velocity in the medium.

Introducing the velocity potential functions ϕ and ψ through the relations

$$u_r = \frac{\partial \phi}{\partial r} + \frac{\partial \psi}{\partial z}, \quad u_z = \frac{\partial \phi}{\partial z} - \frac{\partial \psi}{\partial r} - \frac{\psi}{r}, \tag{3.2}$$

and using Eqs. (3.1)–(3.2) in Eqs. (2.7)–(2.9) and after suppressing the primes for convenience, we obtain

$$\nabla^2 \phi - \frac{\partial^2 \phi}{\partial t^2} + \delta_3^2 \phi^* = 0, \tag{3.3}$$

$$\nabla^2 \psi - \frac{\psi}{r^2} - \frac{\phi_\theta}{\delta^2} - \frac{1}{\delta^2}\frac{\partial^2 \psi}{\partial t^2} = 0, \tag{3.4}$$

$${\delta^*}^2 \nabla^2 \psi = \delta_2^2 \frac{\partial^2 \phi_\theta}{\partial t^2} + 2\delta_2^2 \phi_\theta - \nabla^2 \phi_\theta, \tag{3.5}$$

$$\nabla^2 \phi^* - \delta_4^2 \phi^* - \delta_5^2 \nabla^2 \phi - \delta_6^2 \frac{\partial^2 \phi^*}{\partial t^2} = 0, \tag{3.6}$$

where

$$\nabla^2 = \frac{\partial^2}{\partial r^2} + \frac{1}{r}\frac{\partial}{\partial r} + \frac{\partial^2}{\partial z^2}.$$

The non-dimensional mechanical boundary conditions at $z = \pm d$ are given by

$$t_{zz} = 0,\ t_{zr} = 0,\ m_{z\theta} = 0,\ \lambda_z^* = 0, \tag{3.7}$$

where

$$t_{zz} = \lambda_{0I}\phi^* + (\lambda_I + 2\mu_I + K_I)\frac{\partial u_z}{\partial z} + \lambda_I\Big(\frac{\partial u_r}{\partial r} + \frac{u_r}{r}\Big),$$

$$t_{zr} = \mu_I\Big(\frac{\partial u_r}{\partial z} + \frac{\partial u_z}{\partial r}\Big) + K_I\Big(\frac{\partial u_r}{\partial z} - \phi_\theta\Big),$$

$$m_{z\theta} = \gamma_I \frac{\partial \phi_\theta}{\partial z} + b_{0I}\frac{\partial \phi^*}{\partial r},$$

$$\lambda_z^* = \alpha_{0I}\frac{\partial \phi^*}{\partial z} - b_{0I}\left(\frac{\partial \phi_\theta}{\partial r} + \frac{\phi_\theta}{r}\right).$$

4 Formal Solution of the Problem

We assume the solutions of Eqs. (3.3)–(3.6) of the form

$$(\phi, \psi, \phi_\theta, \phi^*) = [f(z)J_0(\xi r), g(z)J_1(\xi r), w(z)J_1(\xi r), h(z)J_0(\xi r)]e^{-\iota\omega t}, \tag{4.1}$$

where ω is the circular frequency, ξ is the wave number and $J_0(\xi r)$ and $J_1(\xi r)$ are respectively the Bessel functions of order zero and one.

Using Eq. (4.1) in Eqs. (3.3)–(3.6) and solving the resulting differential equations, the expressions for ϕ, ψ, ϕ_θ and ϕ^* are obtained as

$$\phi = (A\cos m_1 z + B\sin m_1 z + C\cos m_2 z + D\sin m_2 z)J_0(\xi r)e^{-\iota\omega t}, \tag{4.2}$$

$$\psi = (A'\cos m_3 z + B'\sin m_3 z + C'\cos m_4 z + D'\sin m_4 z)J_1(\xi r)e^{-\iota\omega t}, \tag{4.3}$$

$$\begin{aligned}\phi_\theta = \delta^2[&(\beta^2 - m_3^2)(A'\cos m_3 z + B'\sin m_3 z)\\ &+ (\beta^2 - m_4^2)(C'\cos m_4 z + D'\sin m_4 z)]J_1(\xi r)e^{-\iota\omega t},\end{aligned} \tag{4.4}$$

$$\begin{aligned}\phi^* = -\frac{1}{\delta_3^2}[&(\alpha^2 - m_1^2)(A\cos m_1 z + B\sin m_1 z)\\ &+ (\alpha^2 - m_2^2)(C\cos m_2 z + D\sin m_2 z)]J_0(\xi r)e^{-\iota\omega t},\end{aligned} \tag{4.5}$$

where

$$m_i^2 = \xi^2(c^2 a_i^2 - 1),\ i = 1,2,3,4; \quad \alpha^2 = \xi^2(c^2 - 1), \quad \beta^2 = \xi^2(\frac{c^2}{\delta^2} - 1),$$

$$\begin{aligned}(a_1^2, a_2^2) = \frac{1}{2}\Big\{&\big[1 + \delta_6^2 - \frac{1}{\omega^2}(\delta_4^2 - \delta_3^2\delta_5^2)\big] \pm \big[\{1 - \delta_6^2 - \frac{1}{\omega^2}(\delta_4^2 - \delta_3^2\delta_5^2)\}^2\\ &+ \frac{4}{\omega^2}\{\delta_4^2 + \delta_6^2(\delta_4^2 - \delta_3^2\delta_5^2)\}\big]^{\frac{1}{2}}\Big\}\end{aligned}$$

$$\begin{aligned}(a_3^2, a_4^2) = \frac{1}{2}\Big\{&\big[\delta_2^2 + \frac{1}{\delta^2} + \frac{\delta^{*^2}}{\omega^2\delta^2}(1 - \frac{2\delta_2^2\delta^2}{\delta^{*^2}})\big] \pm \big[\{\frac{1}{\delta^2} - \delta_2^2 + \frac{\delta^{*^2}}{\omega^2\delta^2}(1 - \frac{2\delta_2^2\delta^2}{\delta^{*^2}})\}^2\\ &+ \frac{4\delta_2^2}{\omega^2\delta^2}\{\delta^{*^2} - 2(\delta^2\delta_2^2 - 1)\}\big]^{\frac{1}{2}}\Big\}.\end{aligned}$$

The displacement components u_r and u_z are obtained from Eqs. (3.2), (4.2) and (4.3) as

$$\begin{aligned}u_r = \big[&-\xi(A\cos m_1 z + B\sin m_1 z + C\cos m_2 z + D\sin m_2 z) + (-A'm_3\sin m_3 z\\ &+ B'm_3\cos m_3 z - C'm_4\sin m_4 z + D'm_4\cos m_4 z)\big]J_1(\xi r)e^{-\iota\omega t},\end{aligned} \tag{4.6}$$

$$\begin{aligned}u_z = \big[&(-m_1 A\sin m_1 z + m_1 B\cos m_1 z - m_2 C\sin m_2 z + m_2 D\cos m_2 z)\\ &- \xi(A'\cos m_3 z + B'\sin m_3 z + C'\cos m_4 z + D'\sin m_4 z)\big]J_0(\xi r)e^{-\iota\omega t}.\end{aligned} \tag{4.7}$$

5 Derivation of the Secular Equations

Invoking the boundary conditions (3.7) on the surfaces z =± d of the plate and using Eqs. (4.2)–(4.7), we obtain a system of eight simultaneous equations.

$$P(AC_1+Bs_1+CC_2+Ds_2)+Q\{m_3(A's_3-B'C_3)+m_4(C's_4-D'C_4)\}=0, \tag{5.1}$$

$$P(AC_1-Bs_1+CC_2-Ds_2)+Q\{m_3(-A's_3-B'C_3)+m_4(-C's_4-D'C_4)\}=0, \tag{5.2}$$

$$Q\{(-As_1+BC_1)m_1+(-Cs_2+DC_2)m_2\}+P(A'C_3+B's_3+C'C_4+D's_4)=0, \tag{5.3}$$

$$Q\{(As_1+BC_1)m_1+(Cs_2+DC_2)m_2\}+P(A'C_3-B's_3+C'C_4-D's_4)=0, \tag{5.4}$$

$$\begin{aligned}&R[g_1C_1A+g_1s_1B+g_2C_2C+g_2s_2D]+S[f_3(-A's_3+B'C_3)m_3\\&\quad+f_4(-C's_4+D'C_4)m_4]=0,\end{aligned} \tag{5.5}$$

$$\begin{aligned}&R[g_1C_1A-g_1s_1B+g_2C_2C-g_2s_2D]+S[f_3(A's_3+B'C_3)m_3\\&\quad+f_4(C's_4+D'C_4)m_4]=0,\end{aligned} \tag{5.6}$$

$$\begin{aligned}&U[g_1(-Am_1s_1+Bm_1C_1)+g_2(-Cm_2s_2+Dm_2C_2)]\\&\quad-V[f_3C_3A'+f_3s_3B'+f_4C_4C'+f_4s_4D']=0,\end{aligned} \tag{5.7}$$

$$\begin{aligned}&U[g_1(Am_1s_1+Bm_1C_1)+g_2(Cm_2s_2+Dm_2C_2)]\\&\quad-V[f_3C_3A'-f_3s_3B'+f_4C_4C'-f_4s_4D']=0,\end{aligned} \tag{5.8}$$

The system of Eqs. (5.1)–(5.8) has a non-trivial solution if the determinant of the coefficients of amplitudes $[A,B,C,D,A',B',C',D']^T$ vanishes. This after lengthy algebraic reductions and manipulations leads to the secular equations for the plate.

$$\begin{aligned}&\left\{1+\frac{QR(m_1^2-\alpha^2)}{PS(m_4^2-\beta^2)}+\frac{QV(m_3^2-\beta^2)}{PU(m_2^2-\alpha^2)}+\frac{Q^2RV(m_1^2-\alpha^2)(m_3^2-\beta^2)}{P^2SU(m_2^2-\alpha^2)(m_4^2-\beta^2)}\right\}\left[\frac{\tan m_1d}{\tan m_3d}\right]^{\pm1}\\&-\left\{\frac{m_1(m_1^2-\alpha^2)}{m_2(m_2^2-\alpha^2)}+\frac{QRm_1(m_1^2-\alpha^2)}{PSm_2(m_4^2-\beta^2)}+\frac{QVm_1(m_3^2-\beta^2)}{PUm_2(m_2^2-\alpha^2)}+\frac{Q^2RVm_1(m_3^2-\beta^2)}{P^2SUm_2(m_4^2-\beta^2)}\right\}\\&\times\left[\frac{\tan m_2d}{\tan m_3d}\right]^{\pm1}-\left\{\frac{m_3(m_3^2-\beta^2)}{m_4(m_4^2-\beta^2)}+\frac{QRm_3(m_1^2-\alpha^2)}{PSm_4(m_4^2-\beta^2)}+\frac{QVm_3(m_3^2-\beta^2)}{PUm_4(m_2^2-\alpha^2)}\right.\\&\left.+\frac{Q^2RVm_3(m_1^2-\alpha^2)}{P^2SUm_4(m_2^2-\alpha^2)}\right\}\left[\frac{\tan m_1d}{\tan m_4d}\right]^{\pm1}+\left\{\frac{m_1m_3(m_1^2-\alpha^2)(m_3^2-\beta^2)}{m_2m_4(m_2^2-\alpha^2)(m_4^2-\beta^2)}\right.\\&\left.+\frac{QRm_1m_3(m_1^2-\alpha^2)}{PSm_2m_4(m_4^2-\beta^2)}+\frac{QVm_1m_3(m_3^2-\beta^2)}{PUm_2m_4(m_2^2-\alpha^2)}+\frac{Q^2RVm_1m_3}{P^2SUm_2m_4}\right\}\left[\frac{\tan m_2d}{\tan m_4d}\right]^{\pm1}\\&-\frac{RV(m_2^2-m_1^2)(m_4^2-m_3^2)}{SUm_2m_4(m_4^2-\beta^2)(m_2^2-\alpha^2)}\left[\frac{\tan m_1d\tan m_2d}{\tan m_3d\tan m_4d}\right]^{\pm1}\end{aligned}$$

$$= \frac{-4\xi^2[1-p/(2\delta^2)]^2 m_1 m_3 (m_2^2-m_1^2)(m_4^2-m_3^2)}{(\beta^2-\xi^2+p\xi^2/\delta^2)^2(m_4^2-\beta^2)(m_2^2-\alpha^2)} \tag{5.9}$$

where

$$P=\beta^2-\xi^2+\frac{p\xi^2}{\delta^2},\ Q=-2\xi(1-\frac{p}{2\delta^2}),\ R=\frac{\xi b_{0I}}{\delta_3^2},\ S=\gamma_I\delta^2,\ U=\frac{\alpha_{0I}}{\delta_3^2},\ V=\xi b_{0I}\delta^2,$$

$$f_i=\beta^2-m_i^2, i=3,4; g_i=\alpha^2-m_i^2, i=1,2; s_i=\sin m_i d, C_i=\cos m_i d, i=1,2,3,4.$$

Here the superscript $+1$ refers to skew symmetric and -1 refers to symmetric modes. Eq. (5.9) is the secular equation for the propagation of modified microstretch viscoelastic waves in the plate. In absence of viscous and stretch effect, the Eq. (5.9) reduces to the equation in micropolar theory of elasticity which is similar as obtained by Eringen [7] after changing the dimensionless quantities to the physical quantities.

Further neglecting the micropolar effect from the resulting equations, the equation reduces to the equation similar as obtained by Graff [9] for classical theory of elasticity and is known as Rayleigh-Lamb equation. The nomenclature has also been used in standard text equation in Ewing *et al.* [8].

Analogous to this equation of classical theory of elasticity, these equations can be recognized as Rayleigh-Lamb Equations for symmetric and anti symmetric waves in an infinite rectangular plate in microstretch viscoelastic solid. We refer to such waves as microstretch viscoelastic plate waves rather than Lamb waves whose properties were derived by Lamb [18] for isotropic elastic solids in elastokinetics. Thus Rayleigh-Lamb type equation also governs circular crested microstretch elastic waves in a plate. Although the frequency wave number relationship holds whether the waves are straight or circularly crested, the displacement, microstretch, microrotation and stresses vary according to Bessel functions rather than trigonometric functions as far as the radial coordinate is concerned. For large value of r, we have

$$J_0(\xi r)\to\frac{\sin\xi r+\cos\xi r}{\sqrt{\pi\xi r}},\quad J_1(\xi r)\to\frac{\sin\xi r-\cos\xi r}{\sqrt{\pi\xi r}}.$$

Thus, far from the origin the motion becomes periodic in r. Actually, "far" occurs rather rapidly, within four to five zeros of the Bessel function. As r becomes very large, the straight crested behavior is the limit of the circular crested waves.

Micropolar elastic Plate

In the absence of viscous effect ($\alpha_{0I}=\lambda_{0I}=\lambda_{1I}=0$) and microstretch effect ($\alpha_0=\lambda_0=\lambda_1=b_0=0$) , the secular equation (5.9) reduces to

$$\left[\frac{\tan m_1 d}{\tan m_3 d}\right]^{\pm1}-\frac{m_3(\beta^2-m_3^2)}{m_4(\beta^2-m_4^2)}\left[\frac{\tan m_1 d}{\tan m_4 d}\right]^{\pm1}=\frac{-4\xi^2(1-p/(2\delta^2))^2\alpha m_3(m_4^2-m_3^2)}{(\beta^2-\xi^2+\frac{p\xi^2}{\delta^2})^2(m_4^2-\beta^2)}. \tag{5.10}$$

The equation (5.10) agrees with Kumar and Partap [13] and has been discussed for homogeneous, isotropic, stress free micropolar elastic plate.

Elastic Plate

In the absence of micropolarity effect ($K = p = 0$), the secular equation (5.10) reduces to

$$\left[\frac{\tan m_1 d}{\tan m_3 d}\right]^{\pm 1} = \frac{-4\xi^2\alpha\beta}{(\beta^2 - \xi^2)^2}. \tag{5.11}$$

The equation (5.11) agrees with Graff [9] and has been discussed for homogeneous, isotropic, stress free elastic plate.

6 Regions of the Secular Equation

In order to explore various regions of the secular equations, here we consider the equation (5.9) as an example for the purpose of discussion. Depending upon whether m_1, m_2, m_3, m_4, α, and β being real, purely imaginary or complex, the frequency equation (5.9) is correspondingly altered as follows:

Region I

When the characteristic roots are of the type, $\alpha^2 = -\alpha'^2$, $\beta^2 = -\beta'^2$, $m_k^2 = -\alpha_k^2$, $k = 1, 2, 3, 4$ so that $\alpha = \iota\alpha'$, $\beta = \iota\beta'$, $m_k = \iota\alpha_k$, $k = 1, 2, 3, 4$ are purely imaginary or complex numbers. This ensures that the superposition of partial waves has the property of exponential decay. In this case, the secular equations are written from equation (5.9) by replacing circular tangent functions of m_k, $k = 1, 2, 3, 4$ with hyperbolic tangent functions of α_k, $k = 1, 2, 3, 4$.

Region II

This region is characterized by $\delta < c < 1$. In this case, we have

$$\beta = \beta, \quad m_3 = m_3, \quad m_4 = m_4, \quad \alpha = \iota\alpha', \quad m_k = \iota\alpha_k, \ (i = 1, 2)$$

and the secular equations can be obtained from equation (5.9) by replacing circular tangent functions of $m_k, k = 1, 2$ with hyperbolic tangent functions of $\alpha_k, k = 1, 2$.

Region III

In this case, the characteristic roots are given by $m_k^2, k = 1, 2, 3, 4$ and the secular equation is given by equation (5.9).

7 Waves of Short Wavelength

Some information on the asymptotic behavior is obtained by letting $\xi \to \infty$, $\tanh \alpha_i d / \tanh \alpha_j d \to 1, i = 1, 2; j = 3, 4$. If we take $\xi > \omega/\delta$, it follows that $c < \delta < 1$.

Then we replace α, β, m_i with $\iota\alpha'$, $\iota\beta'$, $\iota\alpha_i$ and secular equations (5.9) reduces to

$$\begin{aligned}
&4\xi^2(1-\frac{p}{2\delta^2})^2\alpha_1\alpha_2\alpha_3\alpha_4(\alpha_1+\alpha_2)(\alpha_3+\alpha_4)\\
&=(\frac{p\xi^2}{\delta^2}-\beta'^2-\xi^2)^2[(\alpha_1^2+\alpha_2^2+\alpha_1\alpha_2-\alpha'^2)(\alpha_3^2+\alpha_4^2+\alpha_3\alpha_4-\beta'^2)\\
&+\frac{QR}{PS}(\alpha_1^2-\alpha'^2)(\alpha_2^2-\alpha'^2)+\frac{QV}{PU}(\alpha_3^2-\beta'^2)(\alpha_4^2-\beta'^2)\\
&+\frac{Q^2RV}{P^2SU}(\alpha_3\alpha_4+\beta'^2)(\alpha_1\alpha_2+\alpha'^2)-\frac{RV}{SU}(\alpha_1+\alpha_2)(\alpha_3+\alpha_4).
\end{aligned}$$

These are merely Rayleigh surface wave equations. The Rayleigh results enter here since for such wavelengths, the finite thickness plate appears as a half-space. Hence vibrational energy is transmitted mainly along the surface of the plate.

8 Amplitudes of Displacements, Microrotation and Microstretch

In this section, the amplitudes of displacement components, microrotation and microstretch for symmetric and skew symmetric modes of plate waves, have been computed. Upon using Eqs. (4.4)–(4.7), we obtain

$$\begin{aligned}
(u_r)_{sy}&=\{-\xi(\cos m_1z+L\cos m_2z)+Mm_3\cos m_3z+Nm_4\cos m_4z\}AJ_1(\xi r)e^{-\iota\omega t}\\
(u_r)_{asy}&=\{-\xi(\sin m_1z+L'\sin m_2z)+M'm_3\sin m_3z+N'm_4\sin m_4z\}BJ_1(\xi r)e^{-\iota\omega t}\\
(u_z)_{sy}&=-\{m_1\sin m_1z+Lm_2\sin m_2z-\xi(M\sin m_3z+N\sin m_4z)\}AJ_0(\xi r)e^{-\iota\omega t}\\
(u_z)_{asy}&=\{m_1\cos m_1z+L'm_2\cos m_2z-\xi(M'\cos m_3z+N'\cos m_4z)\}BJ_0(\xi r)e^{-\iota\omega t}\\
(\phi_\theta)_{sy}&=\delta^2\{(\beta^2-m_3^2)\sin m_3z-(\beta^2-m_4^2)\frac{f_3m_3C_3}{f_4m_4C_4}\sin m_4z\}B'J_1(\xi r)e^{-\iota\omega t}\\
(\phi_\theta)_{asy}&=\delta^2\{(\beta^2-m_3^2)\cos m_3z-(\beta^2-m_4^2)\frac{f_3m_3s_3}{f_4m_4s_4}\cos m_4z\}A'J_1(\xi r)e^{-\iota\omega t}\\
(\phi^*)_{sy}&=\frac{1}{\delta_3^2}\{(\alpha^2-m_1^2)\cos m_1z+(\alpha^2-m_2^2)L\cos m_2z\}AJ_0(\xi r)e^{-\iota\omega t}\\
(\phi^*)_{asy}&=\frac{1}{\delta_3^2}\{(\alpha^2-m_1^2)\sin m_1z+(\alpha^2-m_2^2)L'\sin m_2z\}BJ_0(\xi r)e^{-\iota\omega t}
\end{aligned}$$

where

$$\begin{aligned}
&L=-\frac{g_1m_1s_1}{g_2m_2s_2},\quad L'=-\frac{g_1m_1C_1}{g_2m_2C_2},\\
&M=\frac{P(g_2m_2T_1^{-1}-g_1m_1T_2^{-1})f_4s_1}{Qg_2m_2m_3(f_4-f_3)T_3^{-1}s_3},\quad M'=\frac{P(g_2m_2T_1-g_1m_1T_2)f_4C_1}{Qg_2m_2m_3(f_4-f_3)T_3C_3},\\
&N=-\frac{P(g_2m_2T_1^{-1}-g_1m_1T_2^{-1})f_3s_1}{Qg_2m_2m_4(f_4-f_3)T_4^{-1}s_4},\quad N'=-\frac{P(g_2m_2T_1-g_1m_1T_2)f_3C_1}{Qg_2m_2m_4(f_4-f_3)T_4C_4},\\
&T_i=\tan m_id,\ i=1,2,3,4.
\end{aligned}$$

9 Example Results

With the view of illustrating theoretical results obtained in the preceding sections, we now present some numerical results. The material chosen for this purpose is aluminium - epoxy composite (microstretch elastic solid), the physical data for which is given below

$$\rho = 2.19 \times 10^3 Kgm^{-3}, \quad \lambda = 7.59 \times 10^9 Nm^{-2}, \quad \mu = 1.89 \times 10^9 Nm^{-2},$$
$$K = 0.0149 \times 10^9 Nm^{-2}, \quad \gamma = 0.0268 \times 10^5 N, \quad j = 0.00196 \times 10^{-4} m^2,$$
$$j_0 = 0.00185 \times 10^{-4} m^2, \quad \lambda_0 = \lambda_1 = 0.037 \times 10^9 Nm^{-2}, \quad \alpha_0 = 0.61 \times 10^5 N,$$
$$b_0 = 0.025 \times 10^5 N, \quad d = 0.01m.$$

For a particular model of a microstretch viscoelastic solid, the relevant parameters are expressed as

$$\chi_I = \chi(1 - \iota Q_k^{-1}),\ k = 1, 2, 3, 4, 5, 6, 7, 8 \text{ for } \chi = \lambda, \mu, K, \gamma, \alpha_0, \lambda_0, \lambda_1, b_0$$

respectively, where

$$Q_1^{-1} = 0.05, \quad Q_2^{-1} = 0.01, \quad Q_3^{-1} = 0.015, \quad Q_4^{-1} = 0.1,$$
$$Q_5^{-1} = 0.15, \quad Q_6^{-1} = 0.15, \quad Q_7^{-1} = 0.1, \quad Q_8^{-1} = 0.1.$$

A FORTRAN program has been developed for the solution of equation (5.9) to compute phase velocity c for different values of n by using the relations $\tan(\theta) = \tan(n\pi + \theta)$ and $m_i^2 = \xi^2(c^2 a_i^2 - 1)$.

In general, wave number and phase velocity of the waves are complex quantities, therefore, the waves are attenuated in space. If we write

$$c^{-1} = v^{-1} + \iota\omega^{-1} q \tag{9.1}$$

then $\xi = K_1 + \iota q$, where $K_1 = \omega/v$ and q are real numbers. This shows that v is the propagation speed and q is attenuation coefficient of waves. Upon using Eq. (9.1) in the FORTRAN program developed for the solution of equation (5.9) to compute phase velocity c, attenuation coefficient q for different modes of wave propagation can be obtained.

The non-dimensional phase velocity and attenuation coefficient of symmetric and skew symmetric modes of wave propagation have been computed for various values of non-dimensional wave number from secular equation (5.9). The corresponding numerically computed values of phase velocity and attenuation coefficient are shown graphically in Figs. 9.1–9.4 for different modes ($n = 0$ to $n = 3$). The amplitudes of displacements, microrotation and microstretch for symmetric and skew symmetric modes are presented graphically in Figs. 9.5–9.12. The solid curves correspond to microstretch viscoelastic plate (MVEP) and dotted curves refer to microstretch elastic plate (MEP).

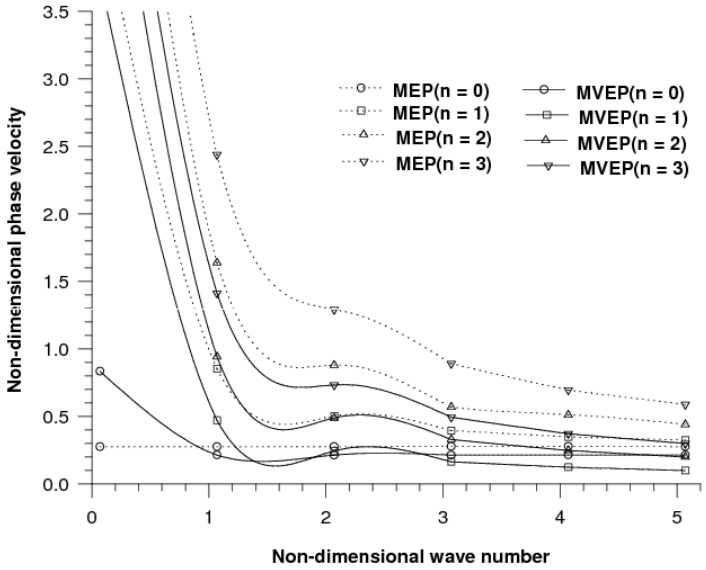

Figure 9.1: Phase velocity profile for symmetric modes of wave propagation

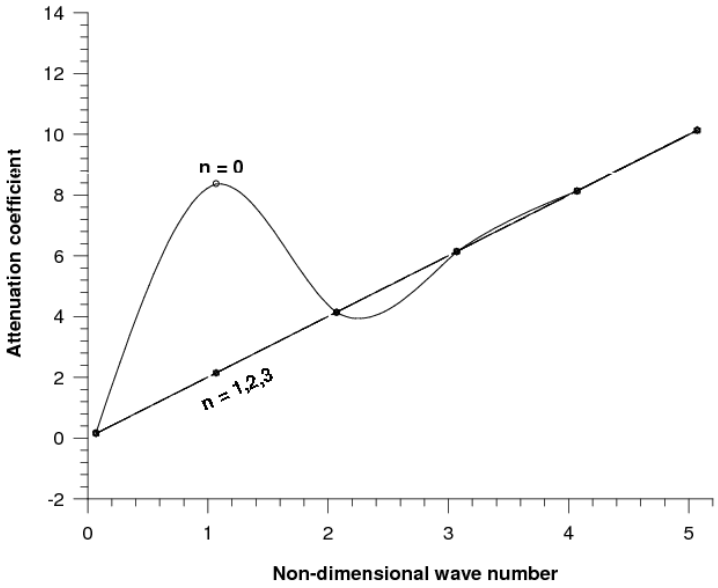

Figure 9.2: Variation of attenuation coefficient of symmmetric modes of wave propagation

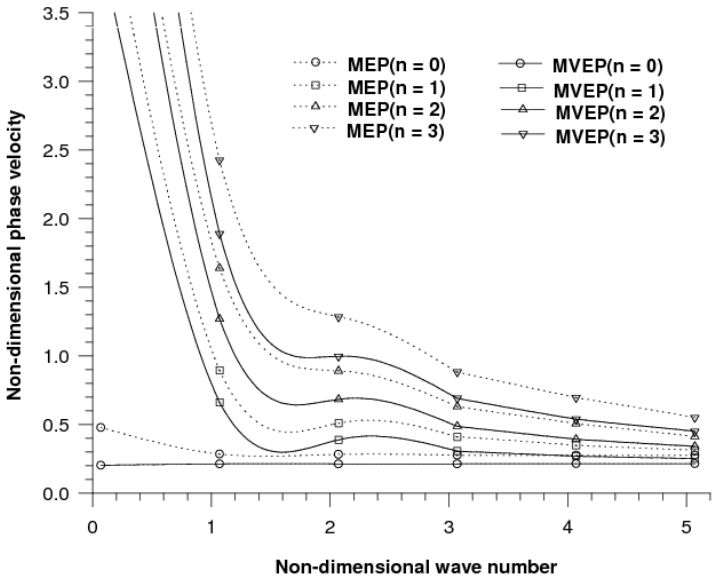

Figure 9.3: Phase velocity profile for skewsymmetric modes of wave propagation

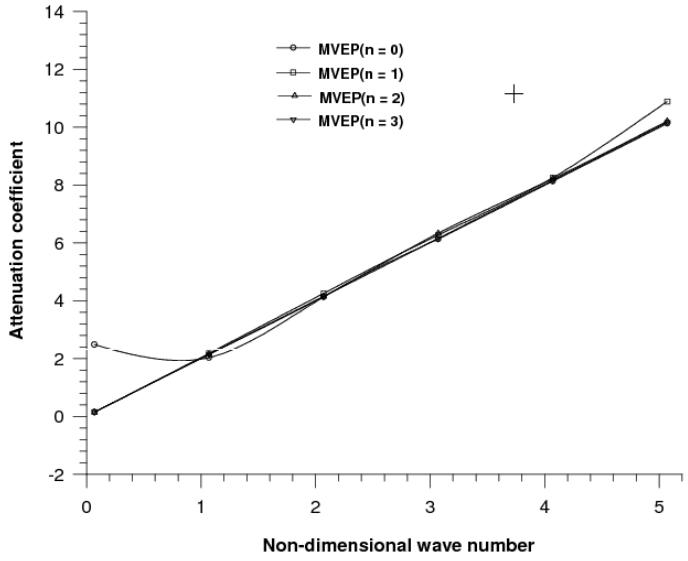

Figure 9.4: Variation of attenuation coefficient of skewsymmmetric modes of wave propagation

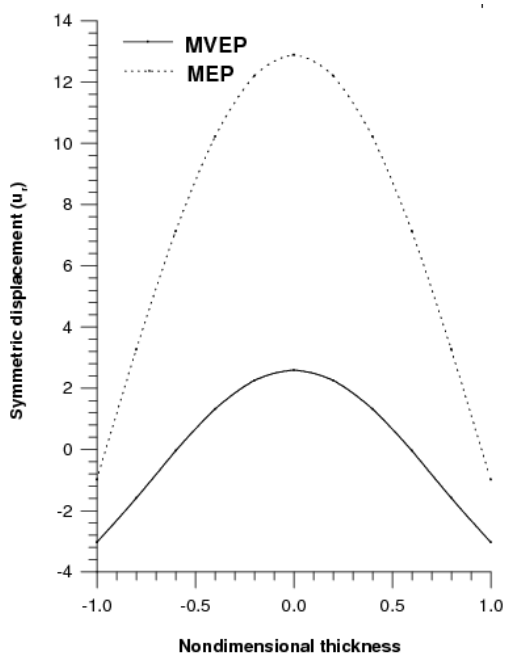

Figure 9.5: Amplitude of symmetric displacement (u_r)

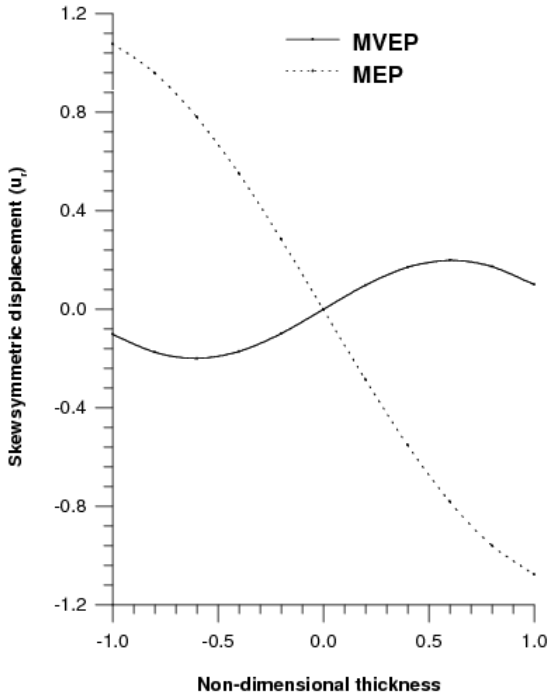

Figure 9.6: Amplitude of skewsymmetric displacement (u_r)

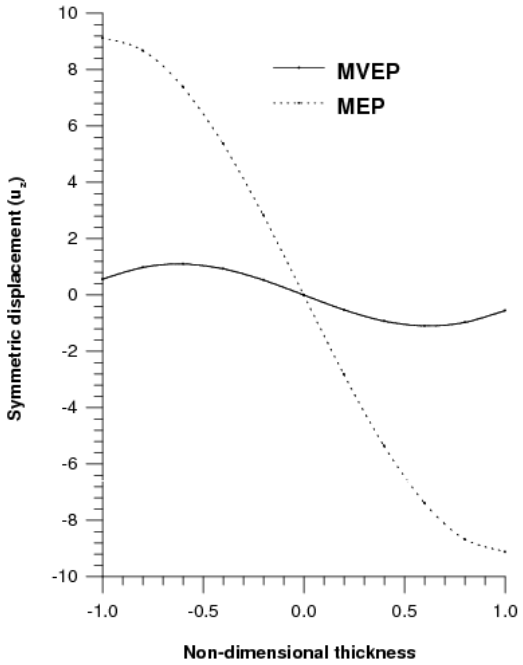

Figure 9.7: Amplitude of symmetric displacement (u_z)

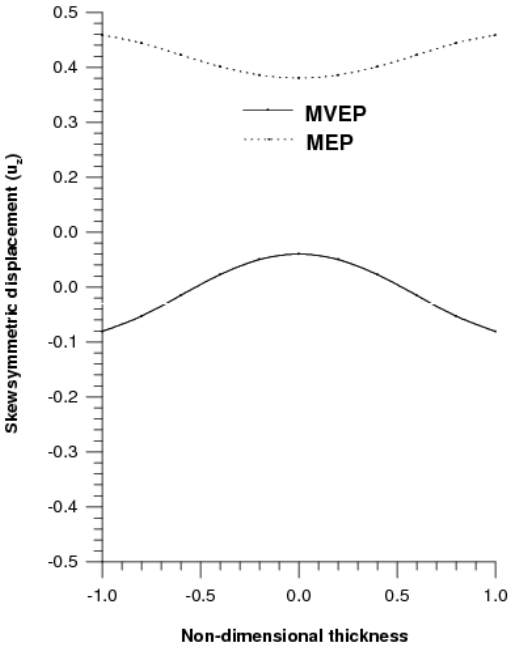

Figure 9.8: Amplitude of skewsymmetric displacement (u_z)

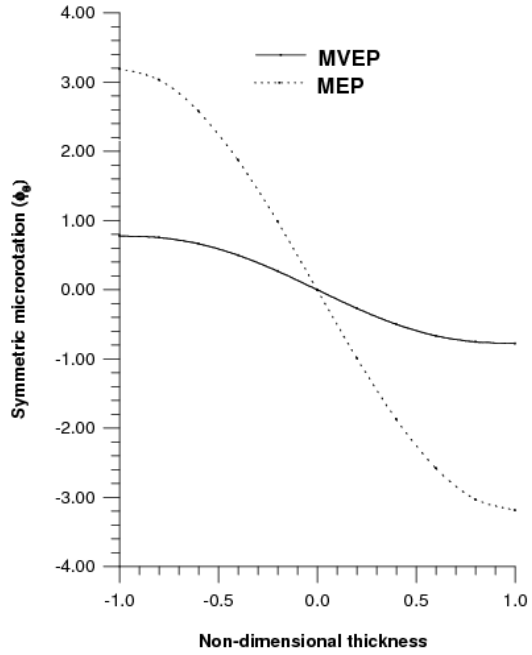

Figure 9.9: Amplitude of symmetric microrotation (ϕ_θ)

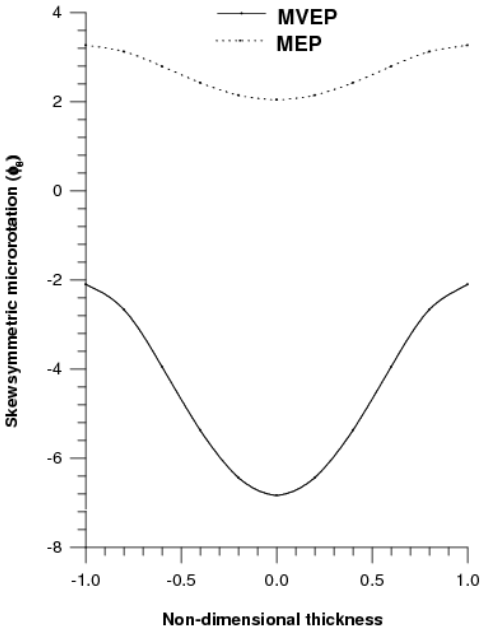

Figure 9.10: Amplitude of skewsymmetric microrotation (ϕ_θ)

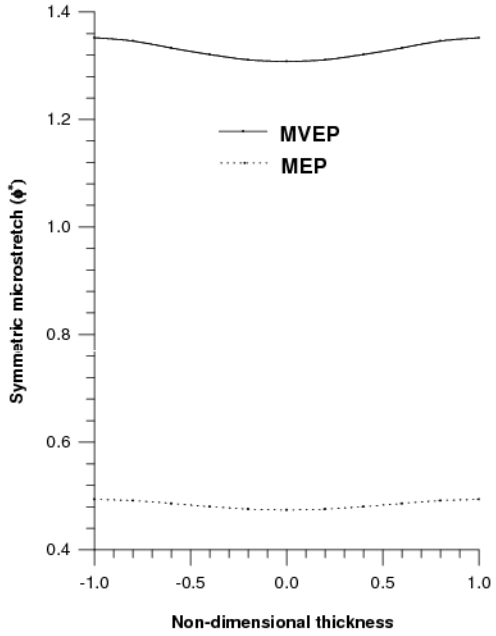

Figure 9.11: Amplitude of symmetric microstretch (ϕ^*)

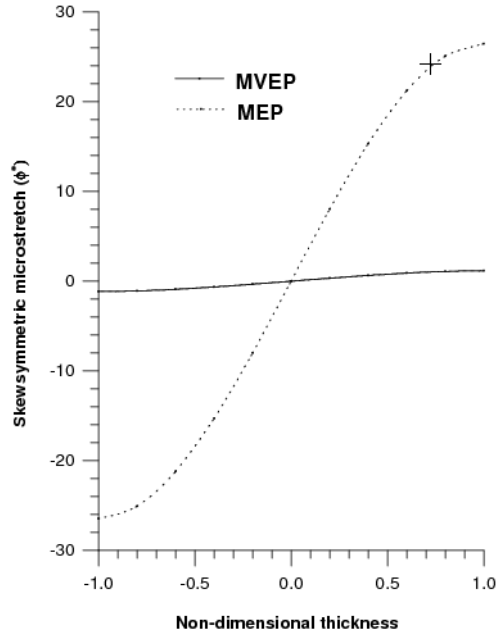

Figure 9.12: Amplitude of skewsymmetric microstretch (ϕ^*)

Phase velocity

The phase velocity of higher modes of wave propagation, symmetric and skew symmetric attains quite large values at vanishing wave number, which sharply slashes down to become steady with increasing wave number. It is observed that the phase velocities of different modes of wave propagation start from large values at vanishing wave number and then exhibit strong dispersion until the velocity flattens out to the value of the microstretch Rayleigh wave velocity of the material at higher wave numbers. The reason for this asymptotic approach is that for short wavelengths (or high frequencies) the material plate behaves increasingly like a thick slab and hence the coupling between upper and lower boundary surfaces is reduced and as a result the properties of symmetric and skew symmetric waves become more and more similar.

The phase velocity of lowest symmetric and skewsymmetric mode ($n = 0$) remains constant with the variation in wave number in microstretch elastic plate (MEP) and microstretch viscoelastic plate (MVEP) respectively, whereas the phase velocity of lowest symmetric mode and skewsymmetric mode ($n = 0$) varies at lower wave number and becomes constant at higher wave number in microstretch viscoelastic plate (MVEP) and microstretch elastic plate (MEP) respectively.

It is observed that phase velocity in MEP is more than in MVEP for symmetric modes $n = 1, 2, 3$ and skewsymmetric modes $n = 0, 1, 2, 3$. In case of lowest symmetric mode ($n = 0$), for wave number $\xi d \leq 0.8$ phase velocity in MVEP is more than in case of MEP, the values of phase velocity are smaller in MVEP than in MEP for wave number $\xi d \geq 0.8$. The phase velocity for symmetric mode $n = 2$ in MEP is more than in case of MVEP for symmetric mode $n = 3$.

Attenuation coefficients

The variation of attenuation coefficient with wave number for symmetric and skew symmetric modes is represented graphically in Figs. 9.2 and 9.4 respectively in case of microstretch viscoelastic plate (MVEP). For the symmetric modes $n = 1, 2, 3$, we observe the following:

(i). the magnitude of attenuation coefficient has maxima upto 10.14 at $\xi d = 5.07$.
(ii). The variation of attenuation coefficient with wave number remains same.
(iii). the attenuation coefficient varies linearly with wave number. For lowest symmetric mode $n = 0$, the magnitude of attenuation coefficient increases upto 8.37 in region $0.07 \leq \xi d \leq 3.08$ at $\xi d = 1.08$ and varies linearly with increase in wave number and attains maxima upto 10.13 in region $3.08 \leq \xi d \leq 5.07$ at $\xi d = 5.07$.

For skewsymmetric modes we observe the following:

(i). the attenuation coefficient varies linearly with wave number for modes $n = 2, 3$.

(ii). for mode $n = 1$, the attenuation coefficient varies linearly with wave number in region $0.07 \leq \xi d \leq 4.08$ and the attenuation coefficient is highest in the region $4.08 \leq \xi d \leq 5.08$ and attains maximum value upto 10.89 at $\xi d = 5.08$.

(iii). for lowest mode, the attenuation coefficient varies linearly with wave number in region $1.08 \leq \xi d \leq 5.08$ and the lowest mode has higher attenuation coefficient than other modes for the region $0.07 \leq \xi d \leq 1.08$.

Amplitudes

Figs. 9.5–9.12 depict the variations of symmetric and skew symmetric amplitudes of displacement (u_r), displacement (u_z), microrotation (ϕ_θ) and microstretch (ϕ^*) in case of microstretch viscoelastic plate (MVEP) and microstretch elastic plate (MEP). The displacement (u_r) of the plate is maximum at the centre and minimum at the surfaces for symmetric mode as can be seen from Fig. 9.5. It is evident from Fig. 9.6 and Fig. 9.7 that (i) the values of the skewsymmetric displacement (u_r) and symmetric displacement (u_z) of the plate is maximum at top surface, zero at the centre and minimum at the bottom surface in case of microstretch elastic plate (MEP); (ii) the values of the skewsymmetric displacement (u_r) is minimum at $z = -0.6d$, zero at the centre and maximum at $z = 0.6d$, whereas the values of the symmetric displacement is maximum at $z = -0.6d$, zero at the centre and minimum at $z = 0.6d$ in case of microstretch viscoelastic plate (MVEP). From Fig. 9.8, it is noticed that the values of the displacement (u_z) of the plate is maximum at the centre and minimum at the surfaces in case of microstretch viscoelastic plate (MVEP) and minimum at the centre and maximum at the surfaces in case of microstretch elastic plate (MEP) for skewsymmetric mode. The values of the symmetric microrotation (ϕ_θ) of the plate is maximum at top surface, zero at the centre and minimum at the bottom surface as seen from Fig. 9.9. The values of the microrotation (ϕ_θ) and microstretch (ϕ^*) of the plate is minimum at the centre and maximum at the surfaces for skewsymmetric mode and symmetric modes respectively as observed from Fig. 9.10 and Fig. 9.11. The values of the skewsymmetric microstretch (ϕ^*) of the plate is minimum at top surface, zero at the centre and maximum at the bottom surface as seen from Fig. 9.12. $(u_r)_{sym}$, $(u_r)_{asym}$, $(u_z)_{sym}$, $(u_z)_{asym}$, $(\phi_\theta)_{sym}$, $(\phi_\theta)_{asym}$, $(\phi^*)_{sym}$ and $(\phi^*)_{asym}$ correspond to the values of (u_r), (u_z), (ϕ_θ) and (ϕ^*) for symmetric and skew symmetric modes respectively. The values of the symmetric displacement (u_r), skewsymmetric displacement (u_z) and skewsymmetric microrotation (ϕ_θ) of the plate are more in microstretch elastic plate (MEP) in comparison to microstretch viscoelastic plate (MVEP), whereas values of the symmetric microstretch (ϕ^*) of the plate are more in microstretch viscoelastic plate (MVEP) in comparison to microstretch elastic plate (MEP). The values of the skewsymmetric displacement (u_r), symmetric displacement (u_z) and symmetric microrotation (ϕ_θ) of the plate are smaller in microstretch elastic plate (MEP) in comparison to microstretch viscoelastic plate (MVEP) below the centre of the plate and are more in microstretch elastic plate (MEP) in comparison to microstretch viscoelastic plate (MVEP) above the centre of the plate, whereas the

values of the skewsymmetric microstretch (ϕ^*) of the plate in case of microstretch elastic plate (MEP) are more below the centre of the plate and are smaller above the centre of the plate.

10 Conclusions

(i). The propagation of axi-symmetric vibrations in infinite homogeneous, isotropic microstretch viscoelastic plate subjected to stress free conditions is investigated after deriving the secular equations.

(ii). It is noticed that the motion of axi-symmetric vibrations is governed by the Rayleigh - Lamb type secular equations.

(iii). At short wavelength limit, the secular equations in case of symmetric and skew symmetric modes of propagation of axi-symmetric vibrations in a stress free plate reduces to the Rayleigh surface frequency equations.

(iv). The phase velocities of higher modes of propagation, symmetric and skewsymmetric attain quite large values at vanishing wave number which sharply slashes down to become steady and asymptotic to the reduced Rayleigh wave velocity with increasing wave number. The phase velocity in MEP is more than in MVEP for symmetric modes $n = 1, 2, 3$ and skewsymmetric modes $n = 0, 1, 2, 3$.

(v). The attenuation coefficient varies linearly with wave number for symmetric modes $n = 1, 2, 3$ and for skewsymmetric modes $n = 2, 3$.

(vi). The amplitudes of displacement components, microrotation and microstretch for symmetric and skew symmetric modes are computed numerically and presented graphically.

References

[1] P. K. Biswas, P. R. Sengupta, and L. Debnath, Axisymmetric Lamb's problem in a semi-infinite micropolar viscoelastic medium, *Comm. Pure Appl. Math.* **19** (1996), 815–820.

[2] S. De Cicco, Stress concentration effects in microstretch elastic solids, *Int. J. Engng. Sci.* **41** (2003), 187–199.

[3] S. De Cicco and L. Nappa, On Saint's Venant's principle for micropolar viscoelastic bodies, *Bit. J. Eng. Sci.* **36** (1998), 883–893.

[4] S. A. EI-Karamany, Uniqueness and reciprocity theorems in generalized linear micropolar thermoviscoelasticity, *Comm. Pure Appl. Math.* **40** (2003), 2097–2117.

[5] A. C. Eringen, Linear theory of micropolar viscoelasticity, *Int. J. Engng. Sci.* **5** (1967), 191–204.

[6] A. C. Eringen, Micropolar elastic solids with stretch, *Ari. Kitabevi Matbassi* **24** (1971), 1–9.

[7] A. C. Eringen, *Microcontinuum Field Theories I: Foundations and Solids*, Springer Verlag, New York, 1999.

[8] M. Ewing, W. S. Jardetzky and F. Press, *Elastic Waves in Layered Media*, McGraw - Hill Book Company, Inc.

[9] K. F. Graff, *Wave motion in Elastic Solids*, Dover publications, New York, 1991.

[10] R. Kumar, Wave propagation in a micropolar viscoelastic generalized thermoelastic solid, *Internat. J. Engrg. Sci.* **38** (2000), 1377–1395.

[11] R. Kumar, M. L. Gogna, and L. Debnath, Lamb's plane problem in micropolar viscoelastic half space with stretch, *Int. J. Math. Math. Sci.* **13** (1990), 363–372.

[12] R. Kumar and G. Partap, Reflection of plane waves in a heat flux dependent microstretch thermoelastic solid half space, *Int. J. of Applied Mechanics and Engineering.* **10** (2005), 253–266.

[13] R. Kumar and G. Partap, Rayleigh Lamb waves in micropolar isotropic elastic plate, *Applied Mathematics and Mechanics* **27** (2006), 1049–1059.

[14] R. Kumar and B. Singh, Reflection of plane waves at a planar viscoelastic micropolar interface, *Indian J. Pure and Applied Math.* **31** (2000), 287–303.

[15] R. Kumar and R. Singh, Elastodynamics of an axisymmetric problem in microstretch viscoelastic solid, *Int. J. Applied Mechanics and Engineering* **10** (2005), 227–244.

[16] R. Kumar, R. Singh, and T. K. Chadha, Axisymmetric problem in microstretch elastic solids, *Indian Journal of Mathematics* **44** (2002), 147–164.

[17] R. Kumar, R. Singh, and T. K. Chadha, Plane strain problem in microstretch elastic solid, *Sadhana.* **28** (2003), 975–990.

[18] H. Lamb, On waves in an elastic plate, *Phil. Trans.Roy. Soc., London, Ser. A* **93** (1917), 114–128.

[19] X. Liu and G. Hu, Inclusion problem of microstretch continuum, *Int. J. Engng. Sci.* **42** (2004), 849–860.

[20] M. F. McCarthy and A. C. Eringen, Micropolar viscoelastic waves, *Int. J. Engng. Sci.* **7** (1969), 447–458.

[21] M. Svanadze, Fundamental solution of the system of equations of steady oscillations in the theory of microstretch elastic solids, *Int. J. Engng. Sci.* **42** (2004), 1897–1910.